SLAC-PUB-2386
August 1979
(N)

RESULTS ON CHARMONIUM FROM THE CRYSTAL BALL*

Presented by C. M. Kiesling (Representing the Crystal Ball Collaboration†)

Stanford Linear Accelerator Center
Stanford University, Stanford, California 94305

† CalTech: R. Partridge, C. Peck, F. Porter.
Harvard University: W. Kollmann, M. Richardson, K. Strauch, K. Wacker.
Princeton University: D. Aschman, T. Burnett, M. Cavalli-Sforza, D. Coyne, H. Sadrozinski.
Stanford University (HEPL): R. Hofstadter, I. Kirkbride, H. Kolanoski, A. Liberman, J. O'Reilly, J. Tompkins.
SLAC: E. D. Bloom, F. Bulos, R. Chestnut, J. Gaiser, G. Godfrey, C. Kiesling, M. Oreglia.

ABSTRACT

Results from the Crystal Ball experiment at SPEAR are presented. A preliminary analysis of the 3 photon final state from the $J/\psi(3095)$ and of the cascade decays of the $\psi'(3684)$ yield new upper limits on the controversial states X(2820), $\chi(3455)$ and the even C-parity state at 3.59 GeV. From inclusive γ-ray spectra of the J/ψ and ψ' preliminary branching ratios for $\psi' \to \chi$ states and upper limits for $J/\psi, \psi' \to \eta_c, \eta_c'$ are given.

1. INTRODUCTION

In the past years it has become evident that certain crucial questions as to the validity of the charmonium interpretation of the narrow resonances J/ψ, ψ' and the states discovered subsequently in e^+e^- can only be answered with a good photon detector. The essential features of such a detector are full coverage of solid angle, high detection efficiency for photons at all energies, good energy resolution and good angular resolution. These features are well approximated by the Crystal Ball Detector System as shown schematically in Fig. 1. Its main components are: (i) a highly segmented shell of NaI(Tℓ) 16 rad. lengths thick covering 94% of 4π (referred to as "the Ball" proper); (ii) a set of cylindrical proportional and magnetostrictive wire chambers inside this shell. The solid angle is extended to 98% of 4π by endcaps of 20 r.l. NaI(Tℓ) behind magnetostrictive wire chambers. The photon detector is supplemented by two muon detectors at 90° to the beam axis (not shown in Fig. 1).

This report presents new (and preliminary) results on exclusive and inclusive reactions and is structured as follows: In Section 2 the detector system is described in detail and its performance during the first half-year of running is reported. Section 3 contains the analysis and the results on the reaction $\psi' \to \gamma\gamma\, J/\psi$, $J/\psi \to \ell^+\ell^-$ and the reaction $J/\psi \to \gamma\gamma\gamma$. In Section 4 initial studies and preliminary results are reported on absolute branching ratios of $\psi' \to \chi\gamma$ and upper limits for the reactions $\psi' \to \gamma\eta_c'$, $\gamma\eta_c$ and $J/\psi \to \gamma\eta_c$ are obtained with ~25% of our final statistics. Finally, some conclusions are drawn on the now changing picture of the existing charmonium states vis-à-vis the results reported.

Presented at the 1979 EPS High Energy Physics Conference,
Geneva, Switzerland, June 27 - July 4, 1979.

* Work supported by the Department of Energy under contract number DE-AC03-76SF00515.

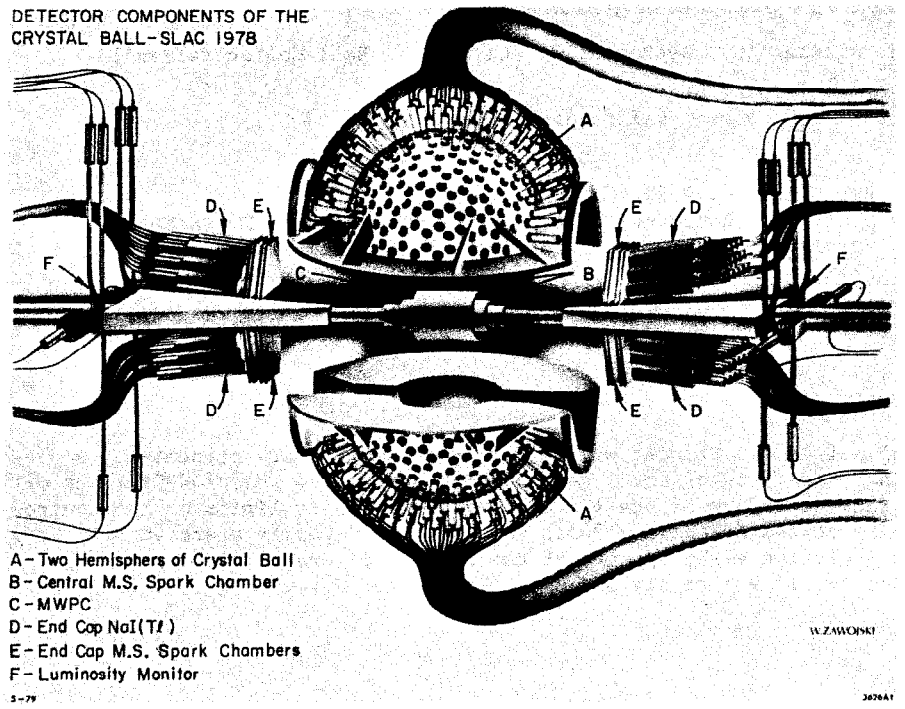

Fig. 1. Schematic representation of the components of the Crystal Ball Detector System.

2. THE CRYSTAL BALL DETECTOR SYSTEM

2.1. Components

The Ball has an outer radius of 66.0 cm and is divided into two hemispheres, each of which is segmented to contain 336 crystals; each crystal is a truncated triangular pyramid. The crystals are optically separated from each other and viewed by individual phototubes. The crystal surfaces are treated in order to give uniform light output (to within ±4%) for a given energy deposition at various points along the crystal.

The beampipe (1.5 mm of aluminum) is surrounded by a set of cylindrical proportional and magnetostrictive wire chambers: the proportional chamber has two gaps with both anode wire and cathode strip read-out and is sandwiched between two double gap magnetostrictive wire chambers. The solid angles subtended are 94% of 4π for the innermost spark chamber, 80% for the proportional chamber and 71% of 4π for the outer spark chamber. The endcaps consist of 4 units of 15 hexagonal crystals (20 rad. lengths of NaI(Tℓ)) each behind 4 gaps of magnetostrictive wire chambers. The solid angle thus covered by NaI and tracking chambers is 98% of 4π. The system is complemented by a luminosity monitor and two muon arms at 90° with respect to the beam axis, each of which consists of 4 arrays of porportional tubes sandwiching iron slabs; the 2 arms subtend a total solid angle of 15% of 4π. These arms will be used for μ-identification and to check the π/e separation capabilities by the ball proper.

Each crystal of the Ball is viewed axially by an SRC L50B01 phototube. Signal readout in the CAMAC-standard electronics involves amplification, integration, holding and an analog multiplexer; all channels are read out sequentially by a fast ADC. The main com-

ponent of the detector trigger is the analog sum of the signals from the Ball, representing the energy deposited in NaI by each event. Energies from subsets of crystals and charged multiplicities (provided by the MWPC) are used in the OR of triggers. More details of the apparatus and triggers are contained in Refs. 1 and 2.

2.2. Performance

The outstanding feature of the Crystal Ball is its energy resolution due to the use of NaI(Tℓ). In a prototype experiment (assembly of 54 crystals) using electrons spanning 50 MeV to 4 GeV in energy, a resolution of

$$\frac{\Delta E}{E}\ (\mathrm{FWHM}) \;=\; \frac{2.8\%}{\sqrt[4]{E(\mathrm{GeV})}}$$

has been achieved[3]. In the actual experiment we presently obtain a resolution worse by roughly a factor of 2. We believe that this discrepancy is mainly caused by changes in time of the calibration between crystals, which we hope to reduce using a light pulser system which we recently developed. The presently used calibration procedure is described in Ref. 4. The angular resolution for photons is $\sim 1.5^{o}$.

In order to check the performance of the entire detector system various QED processes have been measured at different center-of-mass energies. As an example, the process

$$e^{+}e^{-} \rightarrow \gamma\gamma$$

is quoted at the J/ψ and the ψ". At both energies the measured differential cross section (after radiative corrections) agrees with the expected values within the errors of ~5% in an angular acceptance interval of $|\cos\theta| < 0.8$.

3. EXCLUSIVE REACTIONS

A great wealth of results has been accumulated by several experiments on the decays of the J/ψ and ψ'. Nonetheless the candidates proposed for the pseudoscalar states of charmonium are difficult to explain within the framework of the charmonium model[5]. Since most charmonium transitions are accompanied by monochromatic photons, it is not surprising that the Crystal Ball may significantly contribute to the traits and understanding of the charmonium picture.

Results on exclusive decay channels from ψ' reported here are based on the analysis of cascade decays for ~1/4 of the presently available statistics. Results from the reaction $J/\psi \rightarrow 3\gamma$ are based on the full J/ψ statistics of 339 nb^{-1}.

3.1. $\psi' \rightarrow \gamma\gamma\ J/\psi,\ J/\psi \rightarrow \ell^{+}\ell^{-}$

For the analysis of the cascade decays the following event selection criteria have been applied: 4 tracks in the main ball were required with energy depositions per track greater than 20 MeV, 2 of them had to be neutral shower tracks as checked by the central wire chambers and a simple shower recognition algorithm. To ensure that no additional tracks were present in the events an energy deposition of less than 10 MeV in the endcaps was required. In order to minimize the problems arising from overlapping showers, a minimal opening angle between any two tracks of $\cos\theta < 0.9$ was required. The J/ψ in the final state is easily selected in the $e^{+}e^{-}$ decay mode where an invariant mass of

3.1 ± .3 GeV was required for the lepton pair. The $\mu^+\mu^-$ decay channel for the J/ψ was selected by requiring an energy deposition pattern for the two charged tracks characteristic for minimum ionizing particles, i.e., ~200 MeV deposited in 1-3 adjacent crystals. Furthermore, since the μ's stem from the J/ψ, the angle between the minimum ionizing tracks had to be > 140°. Finally two cuts on the photon were applied: the energy sum of the two photons had to roughly match the ψ' - J/ψ mass difference ($E_1 + E_2$ > 480 MeV), and the invariant mass of the two photons should not lie in the η mass region defined by $M_{\gamma\gamma}$ = 549 ± 40 MeV. The overall acceptances for the various cascade processes have been determined by Monte Carlo calculations to range between ~34% and ~48%.

Customarily the cascade reactions are presented in a plot of higher vs. lower (γ - J/ψ) invariant mass, where each of the two γ's is combined with the J/ψ four vector. This two-dimensional plot including ~1/4 of the final statistics is shown in Fig. 2a. It should be noted that the events have not been subjected to kinematic fits. Clearly visible are 2 clusters corresponding to the χ-states of mass 3.55 GeV and 3.51 GeV. The clusters are elongated in the low mass variable indicating the effects of Doppler broadening and NaI(Tℓ) resolution. The high mass combination is observed with the resolution expected from NaI(Tℓ) alone. Thus the excellent energy resolution of the device enables us to easily determine the sequence of the γ-ray emission (i.e., low γ was emitted first). Note furthermore that no pronounced clustering is found in the region of 3.410, 3.455 and 3.6 GeV. The smallness of possible signals at these masses becomes even clearer looking at the high-mass projection in Fig. 2b. No accumulation of events besides the two dominant χ-states is observed. In Table 1 branching ratios for the states χ(3510) and χ(3550) through the cascade process are given and compared with other experiments. The branching ratios for the 3 other states listed in the table should be taken as conservative overestimates as no signal could be established. The well-established χ(3410) state thus seems to have a smaller cascade branching ratio that previously reported by some experiments[6]. Two possible candidates for the η_c' (both the χ(3455) and χ(3591) are only observed in the cascade decays) are not observed in our data. While we wish to refrain from giving upper limits at this stage, we notice that our "signals" at these two masses are significantly lower than the ones claimed by the original experiments[7,8]. New measurements by the Mark II collaboration reported at this conference[10] fail to reproduce the χ(3455) signal which is in agreement with the results presented in this report (see also Table 1). This leaves the χ(3591) for further discussion. We certainly need more statistics to decide about this state. The observed number of events in Fig. 2, however, is at least a factor of 3 below the claimed signal[7].

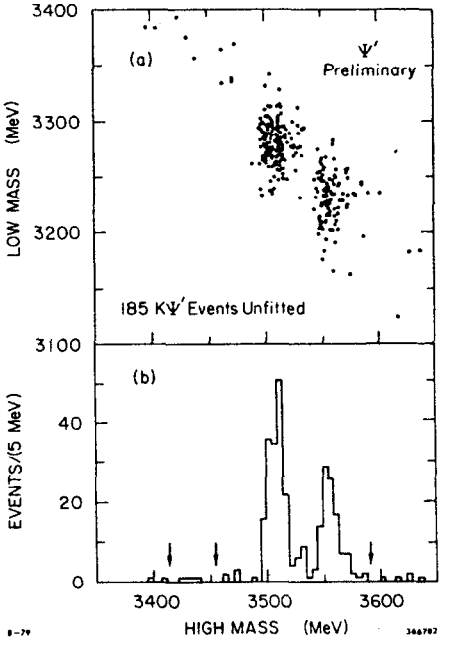

Fig. 2. (a) High mass vs. low mass for the γ - J/ψ mass combination in the ψ' → γγ J/ψ final state. (b) Projection onto the high mass solution.

Table 1

Preliminary Branching Ratios for $\psi \to \gamma\chi$, $\chi \to \gamma\, J/\psi$

χ mass [GeV]	Observed Events	Branching Ratio [%] Other Experiments	This experiment
3.553	104	$1.3 \pm .3$ [a]	$1.3 \pm .3$
3.507	180	$2.3 \pm .4$ [a]	$2.5 \pm .6$
3.409	6 ?	$.14 \pm .09$ [b]	$.1 \pm .06$ [d]
3.455	5 ?	$< .12$ [c]	$.07 \pm .06$ [d]
3.590	6 ?	$.18 \pm .06$ [b]	$.09 \pm .07$ [d]

a) Ref. 8; b) Ref. 7; c) Ref. 10.
d) Caution: no background has been subtracted; for more recent upper limits see Ref. 15.

3.2. $J/\psi \to \gamma\gamma\gamma$

Events of the type $J/\psi \to \gamma\gamma\gamma$ were selected according to the following criteria: Three neutral tracks were required in an angular interval with respect to the beam of $|\cos\theta| \leq 0.8$. The energy deposited for each track had to be ≥ 20 MeV and a minimum opening angle between any two tracks of $\cos\theta_{\gamma\gamma} < 0.9$ was required (as for the cascade events, see above). Since the final state considered consists of 3 showering particles depositing all their energy in the ball, a total energy cut of $2.7 \leq E_{TOT} \leq 3.4$ GeV and a momentum balance cut $\left|\sum_{i=1}^{3} \vec{P}_i\right| < 0.5$ GeV was imposed. A specific background related to the particular angular dimensions of the NaI crystals is due to the reaction $J/\psi \to \gamma\pi^o\pi^o$. This reaction which has similar strength as the 3γ final state may produce two high energetic π^o's $\left(|\vec{P}_{\pi^o}| \gtrsim 1.4 \text{ GeV/c}\right)$. These π^o's in turn decay into two photons with the most likely opening angle of $\sim 15^o$. In general the decay photons will hit two adjacent crystals and form two strongly overlapping showers which will be recognized by the initial event selection as one shower. A closer inspection of the shower patterns, i.e., the energy depositions in crystals close to the shower center, show a characteristic lateral broadening of the shower which in nearly all cases is correlated with another broad shower in the event thus corroborating the hypothesis of the reaction $J/\psi \to \gamma\pi^o\pi^o$ faking a 3γ event. All "broad shower" events were consequently removed from the 3γ sample. Finally, the events were subjected to a 4c kinematic fit with errors for the photon energies and angles as quoted above.

The resulting Dalitz plot for the 411 events satisfying the above selection criteria is shown in Fig. 3. The kinematical boundaries of the Dalitz plot as defined by the cuts as well as the positions of the η and η' bands corresponding to the 2-body reactions $J/\psi \to \gamma\eta,\eta'$ are indicated. Substantial clustering of events around the η and η' bands is observed. The projection of the Dalitz plot onto the low $\gamma\gamma$ mass axis (not the mass squared as in the Dalitz plot proper!) shows clear signals from the $J/\psi \to \gamma\eta,\gamma\eta'$ channels (see Fig. 4a). The high mass projection is shown in Fig. 4b. Most remarkable is the absence of a signal at 2.82 GeV which has been found by the DASP collaboration at DORIS[11]. Assuming our mass resolution of ~25 MeV at 2.8 GeV, one would have expected 53 events in 2

bins above background centered at 2.82 GeV, using the branching ratio quoted in Ref. 11 and taking into account the losses due to the acceptance cuts described above.

In order to determine upper limits for the branching ratio $J/\psi \to \gamma X(X \to \gamma\gamma)$ a likelihood fit to the two-dimensional Dalitz plot incorporating contributions from the reactions $J/\psi \to \gamma\eta$ ($\eta \to \gamma\gamma$), $J/\psi \to \gamma\eta'$ ($\eta' \to \gamma\gamma$), $J/\psi \to \gamma\gamma\gamma$ (direct decay), $e^+e^- \to \gamma\gamma\gamma$ (QED) was performed (the QED contribution has been calculated from first principles and is thus an absolute prediction). Furthermore, the reaction $J/\psi \to \gamma X(X \to \gamma\gamma)$ has been included in the fits assuming masses for the X between 2.7 GeV and 3.04 GeV. No signal could be established in the given mass range. Around 2.82 GeV one arrives at an upper limit for the branching ratio of the reaction $J/\psi \to \gamma X$, $X \to \gamma\gamma$ of $Br(J/\psi \to \gamma X(2820), X \to \gamma\gamma) < 3 \times 10^{-5}$ (90% C.L.) which corresponds to < 6 events above background. The upper limit for an X anywhere in the mass range of 2.7 - 3.04 GeV is $< 5 \times 10^{-5}$.

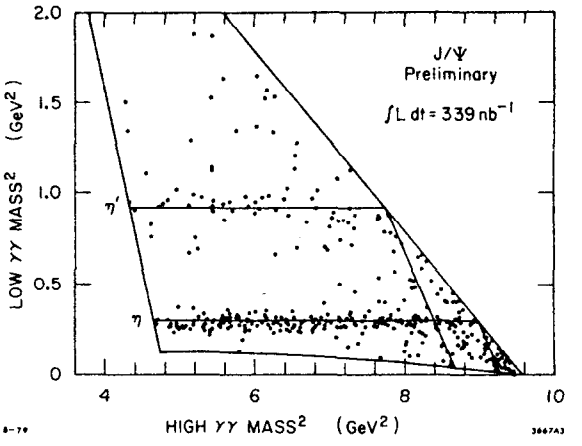

Fig. 3. Dalitz plot for the reaction $J/\psi \to \gamma\gamma\gamma$.

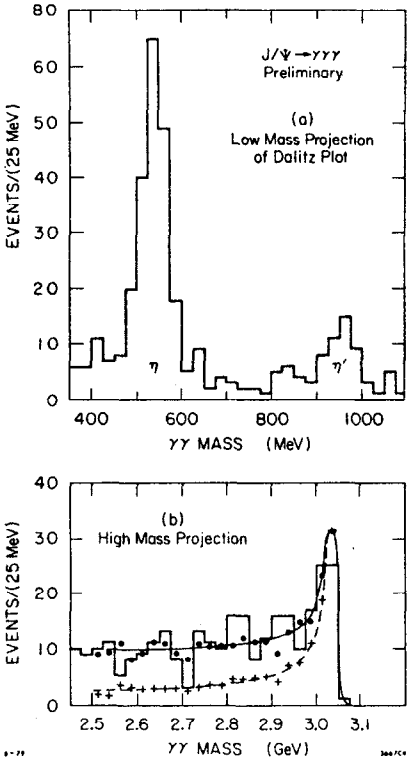

Fig. 4. (a) Projection of the Dalitz plot onto the low mass variable. (b) Projection of the Dalitz plot onto the high mass variable. The solid curve is the result of the likelihood fit to the two-dimensional Dalitz plot as described in the text. The broken line is the predicted contribution from $e^+e^- \to \gamma\gamma\gamma$ (QED).

The curves shown in Fig. 4 are taken from the fit which did not include an X contribution. As a byproduct one obtains the branching ratios for $J/\psi \to \gamma\eta, \gamma\eta'$ which are summarized in Table 2. In contrast to Refs. 11 and 12 on observes a higher yield of η' and a consequently increased ratio of η'/η.

Our experimental upper limits on $\psi \to \gamma\eta_c \to \gamma\gamma\gamma$ can be compared with theoretical predictions: Using the standard result[5] on the η_c branching ratios, the theoretical curve for the overall branching fraction $\psi \to \gamma\eta_c \to \gamma\gamma\gamma$ intersects the experimental upper limit at an η_c mass of 2.975 GeV corresponding to a monochromatic γ-ray of 120 MeV. In other words we can exclude η_c production consistent with the standard assumptions for the charmonium model for η_c masses lower than 2.975 GeV but cease to test them for higher masses (corresponding to lower monochromatic γ-rays).

Table 2

Preliminary Results for the Branching Ratios for $J/\psi \to \gamma\gamma\gamma$ Final States

Decay	Ref. 11	Ref. 12	This Experiment
$J/\psi \to \gamma\eta$	(.82 ± .2)	(1.3 ± 4)	$(1.15 \pm .17) \times 10^{-3}$
$\to \gamma\eta'$	(2.2 ± 1.7)	(2.3 ± .7)	$(6.3 \pm 1.6) \times 10^{-3}$
$\frac{Br(\eta')}{Br(\eta)}$	2.7 ± 2.2	1.8 ± .8	5.5 ± 1.3
$J/\psi \to \gamma X(7820)$	(1.4 ± .4)	< 3.2	$< .3 \times 10^{-4}$
$J/\psi \to \gamma\eta_c$			$< .5 \times 10^{-4}$
$m(\eta_c) \varepsilon [2.7, 3.04\ GeV]$			

4. INCLUSIVE REACTIONS

Probably the most sensitive tool in the search for the charmonium pseudo-scalars consists in the inclusive γ spectra to which each radiative decay of the J/ψ or ψ' would contribute a monochromatic γ-ray irrespective of the decay channel of the coupled system. The disadvantage, however, of the inclusive spectra arises from the expected background under these potential lines since most of the detected photons originate from π^o and η decays. The understanding of this background is crucial in an attempt to maximize the signal/noise ratio, e.g., by means of π^o/η reconstruction and removal of the paired photons.

The preliminary analysis presented here is not yet sophisticated enough to exploit the full power of the Crystal Ball, i.e., to identify those γ's in a general n photon final state originating from π^o/η and derive an energy dependent correction function to account for the subtraction efficiency. Therefore all results quoted subsequently will be derived from the totally inclusive, i.e., unsubtracted photon spectrum. Only angular acceptance cuts for the photons have been imposed ($\cos\theta_\gamma < .71$) in order to make sure that the photon direction was covered by all three central wire chambers.

4.1. Determination of branching ratios for the χ-states

First branching ratios for the three established χ-states and their cascades from the ψ' are determined in order to show the capability of the experiment to measure monochromatic lines using inclusive spectra. A qualitative inclusive spectrum at the ψ' with π^o's removed is shown in Fig. 5. Clearly visible are the three monochromatic lines from ψ' to the χ-states and the Doppler broadened lines from at least 2 χ-states to the J/ψ (see labelling in Fig. 5). The statistics correspond to ~200K ψ' or 1/4 of the full data sample. The line strengths have been obtained by fitting Gaussians to the various peaks superposed on a general polynomial background to the unsubtracted spectrum (not shown).

The results of these fits, corrected for angular acceptance, photon conversion in the beampipe and various other losses are summarized in Table 3. It should be pointed out that the errors are entirely dominated by systematics and therefore have a chance to decrease as the understanding of the apparatus proceeds.

Table 3 displays overall consistency between Ref. 9 (radiative ψ' decays to χ-states), Ref. 8 (cascade decays of the ψ') and this experiment. Note in particular the internal consistency of the cascade branching ratios determined within this experiment from the inclusive spectrum and the cascade process (Section 3.1) itself.

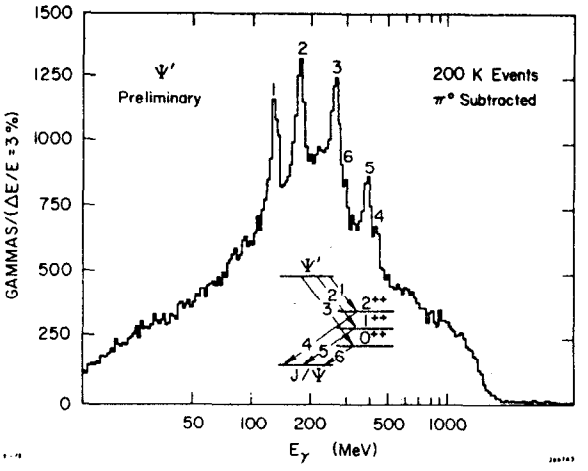

Fig. 5. Inclusive γ spectrum at the ψ'; γ's originating from π^0's have been removed.

Table 3

Preliminary Results on χ Branching Ratios from Inclusive Spectra at the ψ'

Reaction	Branching Ratio [%]	
	Other Experiments	This Experiment
$\psi' \to \gamma\chi(3553)$	7.0 ± 2.0 [a]	7.5 ± 1.7
$\to \gamma\chi(3507)$	7.1 ± 1.9 [a]	7.5 ± 1.7
$\to \gamma\chi(3409)$	7.2 ± 2.3 [a]	7.6 ± 1.7
$\psi' \to \gamma\chi(3507)$, $\chi \to \gamma J/\psi$	$2.3 \pm .4$ [b]	$2.3 \pm .5$
$\psi' \to \gamma\chi(3507)$, $\chi \to \gamma J/\psi$	$1.3 \pm .3$ [b]	$1.5 \pm .4$

a) Ref. 9; b) Ref. 8.

4.2. Search for additional structure

4.2.1. $\psi' \to \gamma\chi$

Besides the prominent lines (with results given in Table 3) no obvious additional structure within our resolution is visible in the ψ' spectrum. A systematic analysis of the γ spectrum has been carried out on the same ψ' data sample as above to determine upper limits for the branching ratios of $\psi' \to \gamma\eta_c'$, $\gamma\eta_c$ for photon energies of $\gtrsim$ 70 MeV* corresponding to η_c' masses of $\lesssim$ 3615 MeV. The procedure to find the upper limits on monochromatic photons as a function of photon energy (using 5 MeV energy steps) follows closely

* We have not yet verified our photon resolution below 70 MeV and thus limit ourselves to higher energies for the time being.

the one outlined above for χ-states. The upper limits for a monochromatic photon at the ψ' fall from ~1.5% at E_γ = 70 MeV to ~0.5% at E_γ = 640 MeV* (excluding, of course, the regions around the χ-states where the 90% C.L. upper limits jump to values around 10%). In particular, at an η_c' mass of 3.59 GeV (see Ref. 7) an upper limit for the branching ratio $\psi' \to \gamma\chi(3.59)$ of 1.4% is measured. The standard prediction[5] of the branching ratio for magnetic dipole transitions at the ψ' intersects the data at an energy for the monochromatic γ-ray of ~120 MeV, i.e., the sensitivity of the presented data is not yet good enough to test the model for level splittings ($\psi' - \eta_c'$) below 120 MeV. The hindered M1 transition $\psi' \to \gamma\eta_c$ with a γ-ray of ~640 MeV predicts a branching ratio of ~0.3% (see Ref. 14), to be compared with the measured upper limit of 0.5%.

4.2.2. $J/\psi \to \gamma\chi$

The unsubtracted J/ψ inclusive spectrum as of now shows no structure which could be associated with a monochromatic γ-ray of measurable size.

Thus upper limits have been determined at the J/ψ in the analogous way as described for the ψ'.

The results are shown in Fig. 6 which displays the upper limit (90% C.L.) for the branching ratio $J/\psi \to \gamma\chi$ based on ~300K J/ψ reactions (~30% of the final statistics) as a function of the photon energy. Also depicted is the prediction using the standard charmonium dipole transitions[5]. Here the crossover point is at ~75 MeV. It is interesting to note that recent calculations incorporating spin-dependent quark forces (Ref. 14) prefer a $J/\psi - \eta_c$ level split around 75 MeV. At the X(2820) the upper limit is down to .4%, a factor of 4 better than a previous determination[9].

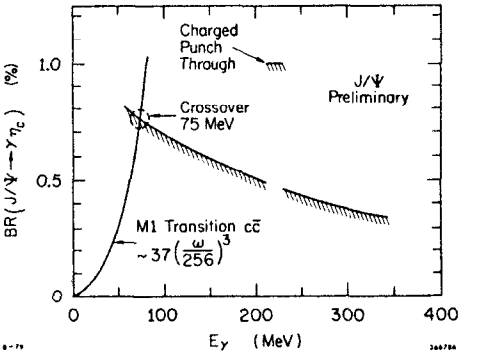

Fig. 6. Upper limit for the branching ratio $J/\psi \to \gamma\eta_c$ as a function of the γ-ray energy. Also shown is the expected yield using the standard model[5].

5. CONCLUSION

The results presented here, although preliminary, strongly suggest a revision of the assignment of charmonium states. While the three χ-states remain established beyond doubt, serious problems seem to arise for the η_c candidate X(2820) and two (alternative!) η_c' candidates at 3.455 GeV and 3.591 GeV. Given the almost optimal capabilities of the Crystal Ball to detect the $J/\psi \to \gamma\eta_c \to \gamma\gamma\gamma$ final state, we consider our upper limits as the death sentence for the X(2820) state. The non-observation of the χ(3455) by both our experiment and the SLAC-LBL collaboration[10] in the cascade mode makes its existence very unlikely. The same can be said for the state observed[7] in the cascade mode at 3591 MeV; due to the low (~90 MeV) energy of the primary photon, the Crystal Ball is the only experiment that can confirm or deny this result. Lack of observation of a 3591 MeV state in both inclusive spectra and cascade decays makes its existence at the level previously published[7] unlikely.

* Due to some low level contamination of the γ spectrum from minimum ionizing particles, the upper limit around 210 ± 20 MeV is ~2%.

The disappearance of the X(2820) and the $\chi(3455)$ is certainly welcome by the proponents of the simpler charmonium model, given the well-known difficulties of the model to fit the large splittings and the transition rates required by the above assignments. The burden of finding the theoretically necessary pseudoscalar partners of the J/ψ and ψ' is still on the experimenters. If the model predictions of the radiative decays of J/ψ and ψ' into η_c and η_c' are roughly correct and the level splittings between $J/\psi - \eta_c$ and $\psi' - \eta_c'$ are no smaller than ~30 MeV (the branching ratios being proportional to E_γ^3), there is a fair chance that these states will be found in the Crystal Ball experiment.†

† Note added in proof:

A preliminary analysis performed after this conference on the π^o subtracted inclusive spectra of the J/ψ and ψ' suggests monochromatic γ-rays from both resonances to a state with a mass around 2977 MeV at a level compatible with the upper limits presented at this conference (see also Ref. 15). This state could be a possible candidate for the η_c.

* * *

REFERENCES

1) E. D. Bloom for the Crystal Ball Collaboration. Invited talk at the XIVth Rencontre de Moriond, 1979. To be published in the Proceedings of the Moriond Conference.

2) J. E. Gaiser et al., Compact Multiwire Proportional Chambers and Electronics for the Crystal Ball Detector. IEEE Trans. on Nucl. Sci., Vol. NS-26, No. 1, 173 (1979).

3) Y. Chan et al., Design and Performance of a Modularized Na(Tℓ) Detector. IEEE Trans. on Nucl. Sci., Vol. NS-25, No. 1, 333 (1978).

4) I. Kirkbride et al., Use of a Low Energy Photon Accelerator for Calibrating a Large Na(Tℓ) Array in a High Energy Physics Experiment. IEEE Trans. on Nucl. Sci., Vol. NS-26, No. 1, 1535 (1979).

5) T. Appelquist, R. M. Barnett and K. Lane, Annu. Rev. Nucl. Part. Sci., Vol. 28, 387 (1978).

6) B. H. Wiik and G. Wolf, DESY Report 23 (1978).

7) W. Bartel et al., Phys. Lett. 79B, 492 (1978).

8) W. M. Tanenbaum et al., Phys. Rev. D17, 1731 (1978).

9) C. J. Biddick et al., Phys. Rev. Lett. 3B, 1324 (1977).

10) J. Weiss, These Proceedings.

11) W. Braunschweig et al., Phys. Lett. 67B, 243,249 (1977).

12) DESY-Heidelberg Collaboration, Proceedings of the 1977 Hamburg Conference, p. 117.

13) W. D. Apel et al., Phys. Lett. 72B, 500 (1978).

14) E. Eichten, F. Feinberg, Preprint HUTP-79/A022 (1979).

15) E. D. Bloom, Report presented at the 1979 International Symposium on Lepton and Photon Interactions at High Energies, Fermi Lab (1979).